AD-A057 062 DELAWARE UNIV NEWARK COLL OF ENGINEERING F/G 7/4
ELECTRO-OPTICAL STUDIES.(U)
MAY 78 K W BOEER N00014-71-C-0169
UNCLASSIFIED NL

1 OF 1
ADA
057062

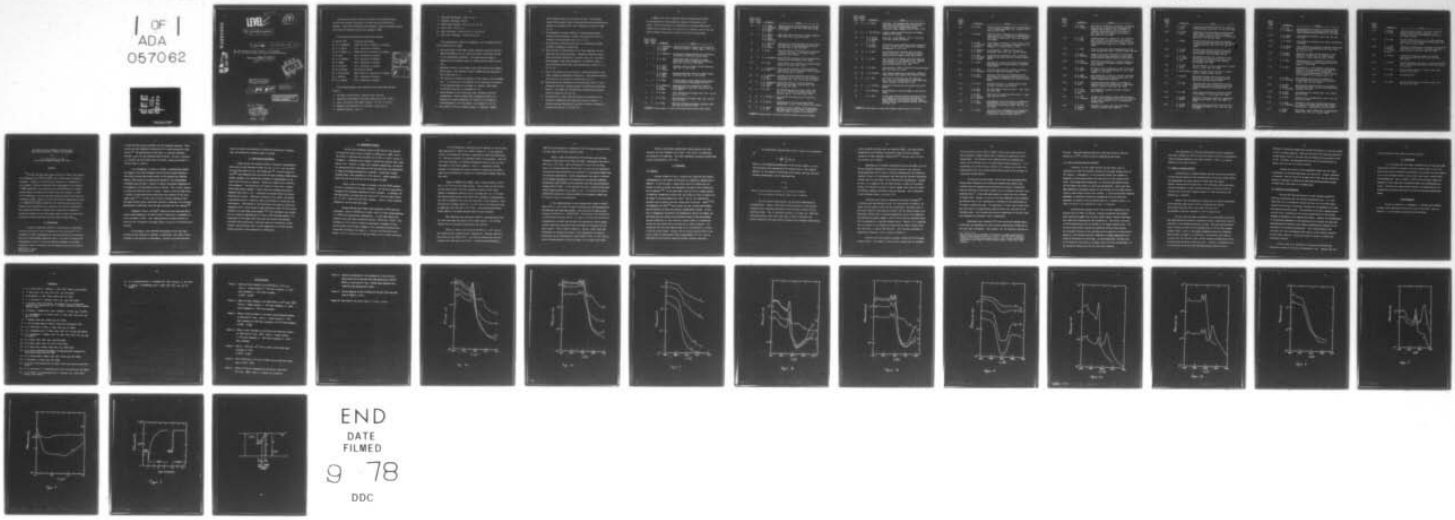

END
DATE
FILMED
9 78
DDC

NR 372-053
Code 427

LEVEL II

19

6 ELECTRO-OPTICAL STUDIES.

9 FINAL REPORT. 1 Nov 70 — 31 Dec 76,

The report covers the time from Nov. 1, 1970 through Dec. 31, 1976 for 6 contract and contract extension periods.

CONTRACT NO. N00014-71-C-0169

15

Department of the Navy
Office of Naval Research
Arlington, Virginia

11 MAY 1978

12 43p.

10 by
K. W. Boer
Principal Investigator
College of Engineering
University of Delaware
Newark, DE 19711

Dept of Physics

409 115

mt

The research performed during the six years of the contract period involved the principal investigator, one Post Doctoral Fellow and ten students. Twenty-five publications were produced. Twenty-one progress reports and thirty-five technical reports were submitted to ONR.

The following researchers were (partially) supported:

Dr. Karl W. Böer	Principal Investigator
Dr. J. A. Bragagnolo	Master and Ph.D., University of Delaware
Dr. G. A. Dussel	Ph.D., University of Delaware
Dr. H. C. Hadley, Jr.	Master and Ph.D., University of Delaware
Dr. P. Voss	Ph.D., University of Delaware
Dr. W. F. Braerman	Ph.D., University of Delaware
Dr. C. Wright	Ph.D., University of Delaware
Dr. G. M. Storti	Ph.D., University of Delaware
Dr. H. M. Windawi	Post Doctoral Fellow
Dr. L. van den Berg	Master and Ph.D., University of Delaware
Dr. J. Phillips	Ph.D., University of Delaware
Dr. W. E. Devaney	Ph.D., University of Delaware

The following subjects were investigated with sponsorship from this contract:

1. CdS single crystal growth: Technical Report (TR) #25.
2. Influences of Ag-doping on electrical properties of CdS: TR #2, 7.
3. Class I and Calss II CdS single crystals: TR #15, 17, 22, 23.
4. Adsorption and desorption of O_2 from CdS: TR #14, 18, 34
5. CdS-Metal Contacts: TR #4, 5

6. Semiconducting glasses: TR #3, 6, 8, 9
7. Ovshinsky switching: TR #10
8. Defect center analysis: TR #1, 13, 18, 19, 31
9. IR detection: TR # 11, 12
10. Solar conversion: TR #16, 20, 26, 27, 28, 29, 35
11. Solar Cells (CdS/Cu_2S): TR #24, 30, 32, 33

The following major tasks were accomplished and are documented in the listed publications or theses:

1. The growth range of CdS single crystal plateletts using the Frerich's method (sublimation in a N_2 - H_2S carrier gas) is described in terms of its thermodynamic parameters. The supersaturation range is analyzed and the parameter range for optimum platelet growth is given (25).
2. Ag-doping introduces deep acceptor states which modifies the recombination traffic. The influence of Ag on recombination and quenching in CdS is described (2, 7).
3. CdS crystals are classified according to their surface - near recombination. It is found that such behaviour can be explained by differences in the (nonstoichiometric) Cd content of a surface - near region of typically less than 1 μm thickenss (17, 22).
4. Oxygen adsorbed at the surface has a major influence on surface recombination. However, whether such recombination shows up in electrical or optical properties is a function of the density of overstoichiometric Cd in the surface - near region (14, 18, 34).
5. The contacts to CdS are injecting (ohmic) or blocking. However,

clean blocking contacts do not block very well. The mechanism involves hole transport near the electrode and carrier generation, and results in a lowering of the work function as a result of light (4, 5).

6. The mechanism for carrier transport in semiconducting glasses involves electron migration in highly perturbed bands and can be explained involving charged defects (3, 6, 8, 9).
7. The switching of Ovshinsky diodes can not be explained by double injection as proposed by others (10).
8. Defect centers in semiconductors are of major importance for most electrical and optical properties. Thermally stimulated currents (TSC) were further analyzed for a specific model, and a new method was developed: Light Induced Modulation of Absorption (LIMA) to obtain information about deep traps (recombination centers) (1, 13, 18, 19, 31).
9. Much of the previous work was devoted to high-field analysis in the range of negative differential conductivity. Here high-field domains occur which can be utilized for IR detection (11, 12).
10. More recently, the utilization of the photovoltaic effect of CdS in combination with Cu_2S, forming an abrupt heterojunction gained major interest. The physics of this effect was analyzed and an improved theory was given (24, 30, 32, 33).
11. The application of solar cells for large scale terrestial use is proposed in combination with thermal harvesting on rooftops. A combined prototype installation, the Solar One House in Delaware is described (16, 20, 26, 27, 28, 29, 35).

A complete list of all technical reports and publications follows. In the first part of this listing, the reports of this contract are listed. Since this contract is a continuation of a previous ONR contract 4336(00) with the same title, the listing of all technical reports from this previous contract follows with a prefix A before the running number.

Techn. Report No.	Status Report No.*	Author(s)	Title
1	1	J. A. Bragagnolo G. A. Dussel K. W. Böer	Thermally Stimulated Currents In The Range Of Unity Gain Factor; Z. Naturf. 26a, 5, 919 (1971)
2	2	H. C. Hadley,Jr.	Ag Doping of Cadmium Sulfide and Its Influence On Electrical Properties, Master Thesis
3	2	K. W. Böer	Second-Order Phase Transition To A High Conductivity State In Semiconducting Glasses; Phys. Stat. Sol.(a) 5, 753 (1971)
4	2	R. J. Stirn K. W. Böer G. A. Dussel	CdS-Metal Contact At Higher Current Densities; Phys. Rev. 7, 1433 (1973)
5	2	G. A. Dussel K. W. Böer R. J. Stirn	Photoconductor-Metal Contact At Higher Current Densities; Phys. Rev. 7, 1443 (1973)
6	2	K. W. Böer	Perturbed Bands In Real Semiconducting Glasses; J. Non-Crystalline Solids 8-10, 586 (1972)
7	3	H. C. Hadley,Jr. P. Voss K. W. Böer	Investigation Of The Influence Of Doping On Field Quenching In CdS; Phys. Stat Sol.(a) 11, K 145 (1972)
8	3	K. W. Böer	Ideal Semiconducting Glasses, Phys. Stat. Sol.(b) 45, K 161 (1971)
9	4	K. W. Böer	Improved Model For Glasses; Phys. Stat. Sol.(b) 47, K 37 (1971)
10	4	K. W. Böer	Ovshinsky Switching And Double Injection; Phys. Stat. Sol.(a) 10, K 31 (1972)

* Number of Status Report in which the Technical Reports were first listed.

Techn. Report No.	Status Report No.*	Author(s)	Title
11	5	R. C. Tyagi J. B. Robertson H. C. Hadley K. W. Böer	Infrared Detection By Reconfiguration Of High Field Domains In CdS; Phys. Stat. Sol.(a) 10, K 57 (1972)
12	6	H. C. Hadley K. W. Böer R. C. Tyagi J. B. Robertson	High Field Domain Solutions In Radial Geometry; Phys. Stat. Sol.(a) 11, 523 (1972)
13	7	W. F. Braerman K. W. Böer G. A. Dussel	Observation Of Deep-Trap Modulation With "Near" Bandedge Light In Copper-Doped CdS Crystals; Pys. Stat. Sol.(a) 35, 309 (1976)
14	8	C. Wright	Desorption Effects On The Electrical Properties Of Class I and Class II CdS Single Crystal Platelets, Ph.D. Thesis
15	9	J. A. Bragagnolo	Effect Of Heat Treatments On The Photoelectronic Properties Of CdS Crystals, Ph.D. Thesis
16		K. W. Böer	Solar Houses To Help Alleviate A Possible Energy Crisis; J. of Chem. Tech. (1973)
17	10	J. A. Bragagnolo K. W. Böer	Effect Of Heat Treatment On The Photoelectric Properties Of Class I CdS Single Crystals; Phys. Stat. Sol.(a) 21, 291 (1974)
18	10	J. A. Bragagnolo C. Wright K. W. Böer	Thermally Stimulated Desorption From Class I CdS Crystals And Its Effect On Their Electrical Properties; Phys. Stat. Sol.(a) 24, 147 (1974)
19	12	J. A. Bragagnolo G. M. Storti K. W. Böer	Bound-Exciton Effects In The Photocurrent Spectrum Of CdS Single Crystals; Phys. Stat. Sol.(a) 22, 639 (1974)
20	14	K. W. Böer	The Solar House And Its Portent; Chem. Tech. Vol. 3, #7, 394-400 (July 1973) Reprinted in Ekistics, 38, No. 225, 96-99 (Aug. 1974)
21	15	H. C. Hadley,Jr.	Quenching Of Photoconductivity In CdS; Ph.D. Thesis
22	15	G. M. Storti	Investigation Of The Near Band Edge Photoconductivity In Class I CdS Crystals; Ph.D. Thesis
23	15	G. M. Storti K. W. Böer	The Effect Of Heat Treatment On The Near Band Edge Photoconductivity Of Class I CdS Crystals (Technical Report attached to this report.)

* Number of Status Report in which the Technical Reports were first listed.

Techn. Report No.	Status Report No.*	Author(s)	Title
24	17	K. W. Böer	Solar One: The Delaware Solar House And Results Obtained During The First Year of Operation; Proc. Intl. Conf. on Photovoltaic Power Generation (DGLR), Hamburg, 627-638 (Sept. 1974)
25	17	L. van den Berg	Growth Of Single Crystal Platelets Of Cadmium Sulfide; Ph.D. Thesis
26	17	D. B. Miller H. M. Windawi K. W. Böer	Solar One: First Results. Part 5: The Solar Electrical System; IEC Report.
27	17	K. W. Böer G. Warfield	Solar Direct Energy Conversion System; Presented at Conf. on Elec. Insul. & Dielectric Phenomena, Downingtown, PA (Oct. 1974)
28	18	K. W. Böer	Solar House System Interfaced With The Power Utility Grid; Proc. Intl. Technical Scientific Meeting on Space, Rome, 397-407 (March 1975)
29	18	K. W. Böer	Solar Electric And Thermal Conversion System In Close Proximity To The Consumer; Proc. AIAA/AAS Solar Energy for Earth Conf., Los Angeles, Paper #75-628 (April 21-24, 1975)
30	19	K. W. Böer	The Photovoltaic Effect In CdS/Cu_2S Heterojunctions; Phys. Rev. B13, 5373 (1976)
31	19	W. F. Braerman	Light Induced Modulation Of Absorption (LIMA) On Copper-Doped Single Crystal CdS Platelets, Thesis
32	21	K. W. Böer	New Results of CdS/Cu_2S Solar Cell Research; Proc. Intl. Conf. on Photovoltaic Power Generation (DGLR), Hamburg, 239-254 (Sept. 1974)
33	21	J. E. Phillips	Electronic Properties Of the Cu_2S-CdS Solar Cell; Thesis
34		W. E. Devaney	Oxygen Adsorption on Photoconductive CdS Surface; Thesis
35		K. W. Böer	A Solar House System Providing Supplemental Energy For Consumers And Peak Shaving With Power-On-Demand Capability For Utilities; Energy: Demand, Conservation and Institutional Problems, MIT Press, 542 (Feb. 1973)

* Number of Status Report in which the Technical Reports were first listed.

Techn. Report No.	Author(s)	Title
A 1	K. W. Böer	Layerlike Field Inhomogeneities in Photoconductors in the Prebreakdown Range, Proc. Semicond. Conf. Paris, p. 987 (1964)
A 2	K. W. Böer	Layerlike Field Inhomogeneities in Homogeneous Semiconductors in the Range of "N-Shaped Negative Differential Conductivity", Phys. Rev. 139, 6A, 1949 (1965)
A 3	K. W. Böer J. C. O'Connell R. Schubert	X-Ray Damage & Annealing of These Defects In CdS Single Crystals, Luminescence Symposium Verl. K. Thiemig, K. G. Munich (1977), p. 223
A 4	P. O. Massicot P. L. Quinn	The Instability of Negative Differential Resistance, Phys. Stat. Sol. 13, K81, (1966)
A 5	K. W. Böer J. C. O'Connell C. A. Kennedy	Production and Annealing of X-Ray and Thermal Damage in CdS Single Crystals, Technical Report ONR #5
A 6	J. J. Ward	High Amplitude Current and Optical Transmission Oscillations in CdS Single Crystals, Technical Report ONR #6
A 7	K. W. Böer J. C. O'Connell	Intrinsic Point Defects in CdS, Pro. Internat'l. Conf. on Luminescence Budapest (1966)
A 8	K. W. Böer P. L. Quinn	Stationary Solutions for Inhomogeneous Field Distribution in Homogeneous Semiconductors In A Range of Negative Differential, Technical Report ONR #8
A 9	R. B. Hall	Electrical Contacts to Cadmium Sulfide Single Crystals, Technical Report ONR #9
A 10	K. W. Böer R. B. Hall	Multilayer Ohmic Contacts on CdS, J. Appl. Phys. 37, 4739 (1966)
A 11	K. W. Böer A. S. Esbitt W. M. Kaufman	Evaporated & Recrystallized CdS Layers, J. Appl. Phys. 37, 2664 (1966)
A 12	K. W. Böer P. L. Quinn	Inhomogeneous Field Distribution in Homogeneous Semiconductors Having An N-Shaped Negative Differential Conductivity, Phys. Stat. Sol. 17, 307 (1966)
A 13	P. L. Quinn	Stationary Field Inhomogeneities in Homogeneous Semiconductors Due to Negative Differential Conductivity, Technical Report ONR #13

Techn. Report No.	Author(s)	Title
A 14	K. W. Böer G. A. Dussell	Time Periodic Solutions of Transport- and Poisson-Equations for Layerlike Field Inhomogeneities, Technical Report ONR #14, later published as Uniformly Propogating Solution of Transport & Poissonequations for Periodic Field Domains, Phys. Rev. 154, 292 (1967)
A 15	K. W. Böer J. J. Ward	Injection Caused p-n Junction in CdS, Technical Report ONR #15, later published as New Kind of Field Instability in CdS in the Range of Negative Differential Resitivity, Sol. St. Commun. 5, 467 (1967)
A 16	J. J. Ward	Study of Layer-Like Field Inhomogeneities in CdS Using Franz-Keldysh Effect, Technical Report ONR #16
A 17	K. W. Böer W. T. Nalesnik	Change of Electrical Conductivity of CdS Single Crystals During Heat Treatments in Sulfur Vapor Between 500° and 700°C, Technical Report ONR #17.
A 18	K. W. Böer J. C. O'Connell	Production and Annealing of Intrinsic Defects in X-ray Irradiated CdS Single Crystals, Technical Report ONR #18
A 19	K. W. Böer J. J. Ward	New Kind of Field Instability in CdS in the Range of Negative Differential Resistivity, Sol. State Communic. 5, 467 (1967)
A 20	K. W. Böer W. T. Nalesnik	Dark Conductivity of CdS as a Function of S-Vapor Pressure During Heat Treatment Between 500° and 700°C, Technical Report ONR #20
A 21	K. W. Böer P. Voss	Stationary High Field Domains in the Range of Negative Differential Conductivity in CdS Single Crystals, Physical Review 171, 899 (1968)
A 22	K. W. Böer G. A. Dussel P. Voss	Field Enhanced Ionization of Traps, Technical Report ONR #22
A 23	K. W. Böer J. C. O'Connell	Intrinsic Point Defects in CdS, Technical Report ONR #23, later published as Intrinsic Point Defects in CdS, Proc. Internat'l Conf. on Luminescence, Budapest (1966)
A 24	K. W. Böer R. Schubert C. Wright	Desorption of Oxygen from Virgin CdS Single Crystals, Technical Report ONR #24

Techn. Report No.	Author(s)	Title
A 25	K. W. Böer P. Voss	Stationary Anode-Adjacent High-Field Domains in Cadmium Sulfide, Phys. Stat. Sol. 28, 355 (1968)
A 26	K. W. Böer P. Voss	Transitions Between Stationary and Moving High-Field Domains in CdS in a Range of Negative Differential Conductivity due to Field Quenching, Phys. Stat. Sol. 30, 291 (1968)
A 27	G. Döhler	Critical Conditions for Transitions Between Stationary and Non-Stationary High Field Domains In Semi-Insulators, Phys. Stat. Sol. 30, 627 (1968)
A 28	K. W. Böer R. Stirn	Effective Work Function of Metal Contacts to Vacuum-Cleaved Photoconducting CdS for High Photocurrents, Technical Report ONR #28
A 29	K. W. Böer G. A. Dussel P. Voss	Experimental Evidence for a Reduction of the Work Function of Blocking Gold Contacts with Increasing Photocurrents in CdS, Physical Review 179,3, 703 (1969)
A 30	K. W. Böer K. Bogus	Electron Mobility of CdS at High Electric Fields, Physical Review 176, 899 (1968)
A 32	L. van den Berg	Growth of Single Crystal Platelets of Cadmium Sulfide, Technical Report ONR #32
A 33	R. Schubert	Desorption of Oxygen and Its Effects on the Electrical Properties of CdS Single Crystal Platelets, Technical Report ONR #33
A 34	K. W. Böer	Trap-Controlled Field Instabilities in Photoconducting CdS Caused by Field-Quenching, IBM Journal of Research and Development 13, 573, (1969)
A 35	K. W. Böer	Light Induced Modulation of Absorption (LIMA) of CdS Crystals, Z. Natf. 24a, 1306 (1969)
A 36	K. W. Böer G. Döhler	Influence of Boundary Conditions on High-Field Domains in Gunn-Diodes, Phys. Rev. 186, 793 (1969)
A 37	K. W. Böer G. Döhler	Temperature Distribution and Its Kinetics in a Semiconducting Sandwich, Phys. Stat. Sol. 36, 679 (1969)

Techn. Report No.	Author(s)	Title
A 38	K. W. Böer W. J. Nalesnik	Semiconductivity of CdS as a Function of S-Vapor Pressure During Heat Treatment Between 500° and 700°C, Materials Research Bulletin 4, 153 (1969)
A 39	G. A. Dussel K. W. Böer	Field Enhanced Ionization, Phys. Stat. Sol. 39, 375 (1970)
A 40	G. A. Dussel	Field Enhanced Ionization, Ph.D. Thesis, Univsersity of Delaware
A 41	G. A. Dussel K. W. Böer	Field Quenching as Mechanism of Negative Differential Conductivity in Photoconducting CdS, Phys. Stat. Sol. 39, 391 (1970)
A 42	R. Schubert K. W. Böer	Desorption of Oxygen and Its Influence on the Electrical Properties of CdS Single Crystal Platelets, J. Phys. Chem. Sol. 32, 71 (1971)
A 44	K. W. Böer	Tunneling Forced by a Temperature Gradient Near the Semiconductor-Electrode Boundaries, Sol. St. Commun. 8, 1329 (1970)
A 45	K. W. Böer	Determination of Field Dependent Conductivity Parameters in Photoconductors Using High-Field Domains, Proceedings of the International Conference on Photoconductivity, (Edit. Erich M. Pell), Pergamon Press, Oxford (1971) p. 75
A 46	K. W. Böer S. R. Ovshinsky	Electrothermal Initiation of an Electronic Switching Mechanism in Semiconducting Glasses, J. Appl. Phys. 41, 2675 (1970)
A 47	K. W. Böer G. Döhler S. R. Ovshinsky	Time Delay for Reversible Electric Switching in Semiconducting Glass, Journal of Non-Crystalline Solids 4, 573 (1970)
A 48	K. W. Böer R. Haislip	Semiconductivity of Glasses, Phys. Rev. Letters 24, 230 (1970)
A 49	K. W. Böer	Remarks to the Ovshinsky Effect, Phys. Stat. Sol. (a) 1, K21 (1970)
A 50	K. W. Böer J. A. Bragagnolo	Luminescence Spectrum of Undoped CdS Platelets as a Function of Slight Heat Treatment in Ultra-High Vacuum, J. Luminescense 1, 2, 572 (1970)
A 51	G. Döhler H. Heike	Concerning a Contact Instability in Semiconductor Diodes, Phys. Stat. Sol. 35, K77 (1969)

Techn. Report No.	Author(s)	Title
A 52	C. Wright K. W. Böer	Transition Between Class I and Class II Crystals Induced by Heat Treatment, Oxygen De-, and Adsorption and Electron Bombardment, Phys. Stat. Sol. 38, K51 (1970)
A 53	K. W. Böer	Electro-Thermal Analysis of a Thin Semi-conducting Sandwich with Field Independent Conductivity, Phys. Stat. Sol.(a) 2, 817 (1970)
A 54	K. W. Böer G. Döhler G. A. Dussel P. Voss	Experimental Determination of Changes in Conductivity with Electric Field Using a Stationary High Field Domain Analysis, Phys. Rev. 169, 700 (1968)
A 55	K. W. Böer	Ideal-Real Semiconducting Glass and Low-High Conductivity Transition, Phys. Stat. Sol.(a) 3, 1007 (1970)
A 56	K. W. Böer	Second Order Phase Transition to a High Conductivity State in Semiconducting Glasses, Phys. Stat. Sol.(a) 5, 753 (1971)
A 57	K. W. Böer	Electro-Thermal Effects in Ovonics, Phys. Stat. Sol.(a) 4, 571 (1971)
A 58	K. W. Böer	Photoconductivity
A 59	K. W. Böer	Electro-Thermal Effects in Ovonics, Phys. Stat. Sol.(a) 4, 571 (1971)

The Effect of Heat Treatment on the Near Band Edge Photoconductivity of Class I CdS Crystals*

by

G. M. Storti+ and K. W. Böer
University of Delaware, Newark, DE 19711

Abstract

The near band edge photocurrent structure of Class I CdS crystals was investigated near 77°K and 295°K by use of double beam illumination techniques. Changes in the photocurrent structure as a consequence of heat treatment, infra-red illumination and oxygen backfill were measured. At 98°K, quenching of the photocurrent near 5000 Å observed in a virgin crystal changed into photocurrent maxima after heat treatment to 175°C. At room temperature, the near band edge quenching remained even after heat treatment to 175°C. Visible and infra-red excitation ranging from 0.6 μm to 1.5 μm (micrometers) always strongly quenched the near band edge photoconductivity maxima but had considerably less influence on the intrinsic photocurrent. The currently-used model to explain Class I properties is expanded to include the influence of the space-charge region in which the photocurrent flows and an acceptor-level with multiply charged energy states.

1. Introduction

A useful classification scheme for characterizing certain photoelectronic properties of CdS was suggested by Gross and Novikov[1] as a consequence of their investigations of the photoconductivity and absorption spectra at liquid nitrogen temperature (LNT). Two types of crystals were distinguished - Class I, in which the spectral dependence of the photoconductivity (SDP) is coincident with the absorption spectrum and Class II

+Part of Ph.D. Thesis
*Supported by ONR

in which the SDP is anti-coincident with the absorption spectrum. These results have been explained satisfactorily in a model presented by Voigt and Ost.[2] The main feature of this model is a position dependent lifetime, $\tau_n(x)$, for the conduction band electrons. In Class I crystals, τ_n is greater near the surface than in the bulk, whereas the reverse is true for Class II crystals.

As a consequence, in Class II crystals, a photocurrent maximum will appear to the long wavelength side of the free exciton absorption lines (the so-called false peak) because of the greater bulk lifetime. However, there should be no photocurrent maximum in the corresponding wavelength range in Class I crystals as long as the spatial dependence of the lifetime is the determining factor in the SDP. This, in fact, appears to be the case with many Class I crystals. However, there are other Class I crystals in which photocurrent maxima have been observed in this wavelength range.[2-7]. In fact, even in Class I crystals showing no near band edge structure under single beam excitation, quenching of an intrinsic photocurrent by additional near band edge excitation has been reported.[8]

Bragagnolo, Storti, and Böer[7] showed that near band edge photocurrent maxima appeared in the SDP of Class I crystals as a consequence of a heat treatment at 180°C. Also, they observed the strong influence of infra-red (IR) illumination and oxygen surface coverage on this photocurrent spectrum.

In this paper, a more detailed investigation of the near band edge photocurrent spectrum is reported. In particular, the effect of heat treatment on the spectrum is investigated. Crystals are probed with both

single and double beam excitation to bring out characteristic features. Also, the influence of adsorbed oxygen is studied.

2. Experimental Arrangement

Single crystal CdS platelets having a thickness of approximately 100 μm and an areal dimension of about 0.5 cm^2 (.5 cm x 1 cm) were grown from the vapor phase in a N_2 - H_2S carrier gas.[9] Two Ti-Al ohmic contacts[10] were evaporated onto one of the two major surfaces [$(11\bar{2}0)$ plane] thereby creating a slit between the electrodes of approximately 0.5 cm across which 20 volts was applied. Current was measured with a Keithley 409 Picoammeter. The photocurrent was excited by light from a tungsten source which passed through a 1-meter Jarrel-Ash scanning spectrometer (spectral band width ≤ 4 Å). A polarizer was placed between the spectrometer and the crystal. Additional excitation of the crystal with either un-polarized visible or infra-red light was provided by a Bausch and Lomb monochromator. Measurements of the photocurrent were made at either room temperature (RT) or near liquid nitrogen temperature (LNT) with the crystal mounted in an ultra-high vacuum chamber.[11] Heat treatments were carried out in a vacuum of approximately 10^{-7} torr in the following fashion: The temperature of the copper block onto which the crystals were pressed (insulated from the block by a thin mica sheet) was increased at a rate between 5 and 10°C/minute until a given temperature was reached and then rapidly quenched to room temperature (∿ 30°C/minute).

3. Experimental Results

The SDP of an untreated crystal at 98°K and 10^{-8} torr excited with polarized light is seen in Figures 1a ($\vec{E}\parallel\vec{C}$) and 1b ($\vec{E}_{\perp}\vec{C}$), curve 1. The effect of step-wise heat treatments up to 175°C is seen in curves 2-4 of Figure 1. Relatively little change in the SDP was observed after treatment at 75°C. However, at higher heat treatment temperatures, the intrinsic photocurrent first decreased and then increased while the photocurrent at longer wavelengths monotonically increased. Considerable changes occurred after a heat treatment at 175°C (curve 4). Maxima appeared at 4900 Å and 4940 Å for $\vec{E}\parallel\vec{C}$ and 4935 Å and 4965 Å for $\vec{E}_{\perp}\vec{C}$.

Figure 2 shows the changes occurring in the SDP ($\vec{E}\parallel\vec{C}$) measured at RT as a consequence of the heat treatments. The intrinsic photocurrent increased with increasing temperature of heat treatment. In addition, the dark photocurrent increased from less than 10^{-12} A for the virgin crystal to $\approx 4 \times 10^{-9}$ A after the 175°C heat treatment. Little, if any, structure appeared in the near band edge range.

Changes observed under double beam excitation at 98°K were very pronounced. Figure 3a ($\vec{E}\parallel\vec{C}$) and 3b ($E_{\perp}C$), curves 1-3 show strong quenching of a 4500 Å bias photocurrent (indicated by -- at the right edge of the figure) by near band edge illumination between $\sim$ 4900 Å and $\sim$ 5100 Å. Heat treatment at 175°C (curve 4) caused the quenching to disappear and two distinct photocurrent maxima to appear at the wavelengths observed in the single beam experiments (see Figure 1). The near band edge photocurrent maxima in curve 4 occurred at the same wavelengths as the strongest quenching.

At room temperature, quenching was also apparent in the near band edge range between ∿ 5000 Å and ∿ 5400 Å (Figure 4). In the untreated crystal, the maximum was centered at approximately 5200 Å for $\vec{E}\|\vec{C}$ (curve 1). With heat treatment, the quenching became less pronounced. After the 175°C heat treatment, the quenching disappeared (curve 4), but was still noticeable in the kinetic behavior - that is, a substantial initial decrease in the photocurrent level occurred on illumination with 5200 A light but was followed by a recovery to a photocurrent slightly above the bias level.

Figure 5a ($\vec{E}\|\vec{C}$) and 5b ($\vec{E}_{\perp}\vec{C}$), curve 1 shows the SDP at ∿ 87°K and 2 x 10^{-3} torr for the virgin crystal. Curve 2 shows the SDP at 87°K for the crystal after 175°C heat treatment, backfill of the vacuum chamber to atmospheric pressure with O_2, and pump down to 2 x 10^{-3} torr. The intrinsic photocurrent levels after heat treatment are approximately one order of magnitude less than they were prior to heat treatment. Also, the post heat treatment levels at ∿ 2 x 10^{-3} torr are an order and a half in magnitude lower than that at 10^{-8} torr. The extrinsic photocurrent maxima remain at the higher pressure after the heat treatment.

With additional bias excitation (4500 Å), some quenching in the near band edge range was present in the virgin crystal. For the heat treated case, the extrinsic photocurrents were additive.

Figure 6, curves 1 and 2 show the RT SDP at 2 x 10^{-3} torr for the virgin and heat treated crystal, respectively. The dark current in both cases was less than 10^{-12} A. The intrinsic photocurrent was considerably less than that at 10^{-8} torr. In double beam measurements, a

4500 Å bias photocurrent was quenched by near band edge illumination both for the virgin and the heat treated crystal.

Figure 7 shows the quenching of the principal near band edge maximum by broad band red and infra-red light. Measurements were made at 87°K and 2×10^{-3} torr. SDP at 87°K and 10^{-3} torr by 0.85 μm light. Curve 1 is without additional IR and curve 2 is with the IR illumination. The near band edge photocurrent was quenched to a much greater degree than the intrinsic photocurrent. Further measurements were made to determine the wavelength dependence of the quenching of the B_1 exciton intrinsic photocurrent (4850 Å $\vec{E}11\vec{C}$) and the principal near band edge photocurrent maximum (4933 Å, $\vec{E}11\vec{C}$). It was observed that the B_1 exciton photocurrent showed slight quenching in the range 0.6 μm to 1.1 μm while the 4933 Å photocurrent maximum was strongly quenched by wavelengths ranging from 0.6 μm to at least 1.5 μm (Figure 8).

It was found necessary to pre-illuminate the crystal at 4933 Å (E11C, 87°K, 2×10^{-3} torr) in order to develop fully the photocurrent of the principal near band edge maximum. This could not be done by prior intrinsic illumination ($\lambda < 4860$ Å, $\vec{E}11\vec{C}$). The build-up of the photocurrent at 4933 Å required several minutes. If, then, the crystal was intrinsically illuminated for one-half-hour and then re-illuminated at 4933 Å, photocurrent steady state occurred at this wavelength of excitation in less than a minute. This is shown in Figure 9. However, either infra-red illumination or warming the crystal to room temperature was found to necessitate the pre-illumination at 4933 Å ($\vec{E}11\vec{C}$, 87°K, 2×10^{-3} torr) to restore the photocurrent at this wavelength to its steady state value.

Finally, the intrinsic photocurrent varied linearly with light intensity for heat treatments up to 125°C. Above 125°C, the dependence was observed to be sublinear. The linear dependence returned on backfilling with O_2 and pump-down to 10^{-3} torr.

4. Discussion

4.1 General

Previous studies on Class I crystals have indicated that spatial inhomogeneities in the defect distribution are required to explain Class I behavior. On the one hand, a higher donor density is needed near the surface in order to explain the substantial increase in dark current with heat treatments.[12] On the other hand, there has to be a higher density of effective recombination centers near the surface in order to explain the the shape of the photoconductivity curve - that is, the lifetime for electrons must be greater near the surface than in the bulk. Weber[13,14] and Bragagnolo and Böer[11] have treated the case in which band bending near the surface provides the necessary recombination centers. In this case, a homogeneous distribution of recombination centers is assumed, but only those near the surface are sensitized because of the band bending. The other possibility is that there are a greater number of recombination centers near the surface than in the bulk due to growth conditions. The experiments that have been reported above do not differentiate as to which of the two is most likely. However, they do indicate that the width of the layer in which the photocurrent flows is approximately 10^{-5} cm - that is, approximately the extinction length for maximum intrinsic absorption.

The photocurrent obtained from a Class I crystal can be expressed as

$$I = \frac{e\mu FA}{L} \int_0^L n(x)\, dx$$

where x is the dimension perpendicular to the crystal surface, A is the cross-sectional area through which the current flows, μ, the electron mobility, F, the electric field between the contacts, and n(x), the free electron concentration, can be determined from

$$n = a\tau_n$$

$$\partial = \beta k I$$

where a is the excitation density, τ_n, the electron lifetime.

For the subsequent discussion, steady state is assumed.

For the intrinsic photocurrent, the excitation mechanisms are straightforward - namely, either band to band excitation or free exciton absorption with subsequent ionization of the electrons and holes to the respective bands. This is indicated as process 1 in Figure 10. Near band edge photocurrents (other than those seen in Class II crystals) are usually associated with bound exciton formation with subsequent dissociation

of the electrons and holes into the respective bands. The bound exciton mechanism has the advantage of potentially high oscillator strengths (reflected in high absorption coefficients)[15] and deep levels at which the excitons can be formed.

Quenching of an intrinsic photocurrent by near band edge excitation and the subsequent appearance of photocurrent maxima on heat treatment having magnitudes close to that of intrinsic photocurrents (for absorption constants likely to be considerably less than that for intrinsic absorption) indicate that the excitation is also affecting the recombination. Because of this, it is suggested that the bound exciton is formed at an acceptor. Further, the acceptor can exist in various charge states that are located at different energetic positions within the band gap. (For a discussion of multi-charged centers, see Ryvkin.[16])

Following ideas initially formulated by Halsted and Segall[17] to explain green edge emission in CdS, the bound exciton is formed at the singly ionized acceptor levels and then dissociates, releasing a hole to the valence band and converting the acceptor intc the doubly-ionized state. The doubly ionized state is located energetically close to the conduction band (Halsted and Segall suggest a level 0.09 eV from the conduction band), but is surrounded by a repulsive coulomb barrier. However, it is suggested that an electron can be thermally released from the doubly ionized center into the conduction band at LNT and above. This excitation mechanism is indicated by processes 2 and 3 as shown in Figure 10.

Electrons and holes normally recombine through the multi-charged acceptor levels. For example, a hole from the valence band can recombine

with an electron in the singly or doubly ionized state converting it to the un-ionized or singly ionized state, respectively (processes 4 and 5, respectively). The electron in the conduction band can recombine and convert the un-ionized state to a singly-ionized state (process 6). It is considerably less likely that an electron will recombine and convert the singly-ionized state to a doubly-ionized state because of the presence of a repulsive coulomb barrier.

On the basis of these ideas, the near band edge quenching occurs because holes produced by the excitation recombine more rapidly with electrons from the conduction band (provided by intrinsic illumination) than the electrons in the doubly ionized state are thermally excited to the conduction band.* A near band edge maxima will appear when this criteria no longer holds. However, it can be of the same magnitude as the intrinsic photocurrent only if the recombination is modified by the deactivation of the normal recombination path. The appearance of a hole trap on heat treatment can result in a significantly greater lifetime for electrons in the conduction band. Hole trapping and electron recombination at the hole trap are represented by processes 7 and 8, respectively.

Chemeresyuk and co-workers[20-22] have noted both negative photoconductivity and quenching of a bias intrinsic photocurrent in CdSe due to near band edge illumination. This suggests that the phenomena involved are

*This criteria must be fulfilled if quenching of a bias photocurrent in negative photoconductivity[18] is to occur. Bube[19] points out that conditions for negative photoconductivity are most easily fulfilled by centers that have singly or doubly charged negative states for n-type material.

the same. Transient quenching behavior as observed by them in CdSe and Gutsche et. al.[22] in CdS can also be explained by this model.

4.2 Effect of Vacuum and Heat Treatment

Initially, for the virgin crystal, the dark Fermi level is positioned very near the energetic position of the singly charged state of the acceptor. Consequently, in the unexcited crystal, the acceptor is primarily in the un-ionized state with some centers in the singly-ionized state. With single beam illumination, the intrinsic photocurrent levels are low because the crystal is relatively unsensitized. Little near band edge quenching is observable because of the relative lack of singly ionized states at which bound excitons can be formed. A linear photocurrent-intensity dependence is observable because the illumination does not affect the population of centers in the un-ionized state (τ_n = constant since p_r, the density of holes in the recombination centers, is constant).

Decreasing the pressure to 10^{-8} torr and heat treatments at this pressure have the effect of driving electrons associated with adsorbed gases (primarily oxygen) into the near surface region, thereby sensitizing this region and increasing the dark conductivity. This causes a decrease in the un-ionized states and an increase in the singly ionized states. The intrinsic photocurrent increases and quenching effects become greater. The subsequent decrease of the quenching and the appearance of photocurrent maxima at $\sim$ LNT indicate that heat treatments at higher temperatures have caused the formation of a hole trap. At room temperature, the hole trap is not effective (the trap is in thermal contact with the valence band), so that quenching remains even for the 175°C heat treatment.

The appearance of a non-linear photocurrent-intensity dependence after heat treatment at 175°C is due to the number of holes in recombination centers becoming dependent on the light intensity - that is, τ_n becomes dependent on the light intensity.

4.3 Effect of Oxygen Backfill

Reintroduction of oxygen decreases the dark current and the intrinsic photocurrent because of the de-sensitization of the near surface region. The chemisorption of oxygen removes electrons from this region, thereby lowering the dark Fermi level. The linear photocurrent-excitation intensity dependence is again observable because the density of the un-ionized state of the multi-charged acceptor is little affected by illumination (τ_n = constant).

However, the reintroduction of oxygen does not affect the presence of the near-band edge maxima at LNT in the photocurrent spectra. This further indicates that a new center, the hole trap, was produced by the heat treatment at 175°C in high vacuum.

The fact that prolonged illumination at the wavelength of the near band edge photocurrent maxima is required to obtain a steady-state value is indicative of the competing processes involved. Near band edge excitation tends to reduce the density of un-ionized states of the multiply charged acceptor levels - that is, the normal recombination path for conduction band electrons no longer is as effective. The excitation also tends to re-route holes into the hole traps, thereby enhancing recombination of the conduction band electrons through this path. Intrinsic illumination prior to the build-up of the near-band edge photocurrent maxima is not as

effective in producing trapped holes because the density of un-ionized states is not as strongly affected. After the build-up of the near-band edge photocurrent maxima, holes in the hole traps can remain for long periods of time at LNT. Therefore, the subsequent build-up time of the photocurrent is shorter than that for the initial build-up.

Heating the crystal to room temperature ionizes the hole traps. Consequently, no near-band edge maxima are seen at RT. Instead, quenching is observed. When the crystal is brought back to LNT, the same excitation process is necessary to build-up the near band edge photocurrent maxima; in other words, holes have to be trapped again.

4.4 Effect of IR Illumination

The near-band edge photocurrent was more strongly quenched by infra-red illumination than the intrinsic photocurrent was. It is most likely that the IR illumination excites the holes out of the hole traps, thereby de-activating a key process necessary for the appearance of a near-band edge photocurrent maxima. The prevention of the hole trapping process can also cause a quenching of the intrinsic photocurrent if the electron lifetime is dependent on the trapped hole density. However, the dissimilarity of the spectral dependence of the quenching of the intrinsic and near-band edge photocurrents indicates that another mechanism may be dominant in the quenching of the intrinsic photocurrent. This could possibly be the activation of a fast recombination path similar to that commonly reported for CdS single crystals. Further work needs to be done to clarify the transitions involved.

The fact that it is necessary to build-up the near band edge photocurrent maxima at LNT after IR illumination also supports the idea

of the existence of hole traps after heat treatment.

5. Conclusions

It is concluded that the defect responsible for the near band edge photocurrent behavior is located in the near surface region ($\simeq 10^{-5}$ cm). Both excitation and recombination processes are associated with this defect. It is a multi-charged acceptor with at least three states located within the forbidden gap. Heat treatment at 175^{o}C and low pressure causes the formation of hole traps that considerably modify the recombination processes. Adsorption of oxygen further enhances the modification of the recombination processes associated with the near band edge photocurrent maxima.

Acknowledgments

We wish to thank Drs. J. Bragagnolo, J. Phillips and H. Hadley for many useful discussions during the course of this work. Also, we thank Dr. L. van den Berg for growing the CdS platelets.

References

1. E. F. Gross and B. V. Novikov, J. Phys. Chem. Solids, 22, 87 (1961)
2. J. Voigt and E. Ost, Phys. Stat. Sol., 33, 381 (1969).
3. H. Mitsuhaski, J. Phys. Chem. Solids, 22, 223 (1961).
4. Y. S. Park and D. C. Reynolds, Phys. Rev., 132, 2450 (1963).
5. Y. Fujishvio and H. Mitsuhashi, Proceedings of the International Conference on Luminescence, Ed., G. Szigeti, Akadémiai Kiadó, Budapest 1968 (p. 1056).
6. K. Colbow, A. Jmaeff and K. Yuen, Canadian J. of Phys. 48, 57 (1970).
7. J. A. Bragagnolo, J. M. Storti, and K. W. Böer, Phys. Stat. Sol. (a) 22, 639 (1974).
8. L. Grabner, Phys. Rev. Letters 14, 551 (1965).
9. L. van den Berg, Master's Thesis, University of Delaware, 1972.
10. K. W. Böer and R. B. Hall, J. Appl. Phys. 22, 75 (1966).
11. J. A. Bragagnolo and K. W. Böer, Phys. Stat. Sol. (a) 21, 291 (1974).
12. J. A. Bragagnolo, C. Wright, and K. W. Böer, Phys. Stat. Sol. (a), 24, 147 (1974).
13. E. H. Weber, Phys. Stat. Sol., 28, 649 (1968).
14. E. H. Weber, Phys. Stat. Sol. (a) 1, 665 (1970).
15. C. H. Henry and K. Nassau, Phys. Rev. B 1, 1628 (1970).
16. S. M. Ryvkin, Photoelectric Effects in Semiconductors, Chapter VII, Consultants Bureau, New York 1964.
17. R. E. Halsted and B. Segall, Phys. Rev. Letters 10, 392 (1963).
18. F. Stockmann, Z. Physik 143, 348 (1955).
19. R. H. Bube, Photoconductivity of Solids, John Wiley and Sons, New York (1960).
20. T. Ya. Sëra and G. G. Chemersoyuk, Sov. Phys. Solid State 6, 104 (1964).
21. T. Ya. Sëra, G. G. Chemersoyuk and V. N. Duldier, Sov. Phys. Solid State 6, 3015 (1965).

22. G. G. Chemeresyuk and V. V. Serdyuk, Sov. Phys. Semicond. 1, 320 (1967).

23. E. Gutsche, F. Spiegelberg, and J. Voigt, Phys. Stat. Sol. 17, K11 (1966).

Figure Captions

Figure 1. Effect of heat treatment on the 98°K SDP at $\sim 10^{-8}$ torr. Curve 1: virgin crystal; 2: 75°C heat treatment; 3: 125°C heat treatment; 4: 175°C heat treatment.
a) $\vec{E} \| \vec{C}$ b) $\vec{E}_{\perp} \vec{C}$

Figure 2. Effect of heat treatment on the 295°K SDP at $\sim 10^{-8}$ torr. $\vec{E} \| \vec{C}$ Curve 1: virgin crystal; 2: 75°C heat treatment; 3: 125°C heat treatment; 4: 175°C heat treatment.

Figure 3. Effect of heat treatment on the double beam excitation results at 98°K and 10^{-8} torr. Curve 1: virgin crystal; 2: 75°C heat treatment; 3) 125°C heat treatment; 4) 175°C heat treatment.
a) $\vec{E} \| \vec{C}$ b) $\vec{E}_{\perp} \vec{C}$

Figure 4. Effect of heat treatment on the double beam excitation results at 295°K and 10^{-8} torr. $\vec{E} \| \vec{C}$. Curve 1: virgin crystal; 2: 75°C heat treatment; 3: 125°C heat treatment; 4: 175°C heat treatment.

Figure 5. SDP at $\sim$ 87°K and $\sim 10^{-3}$ torr 1) before and 2) after heat treatment to 175°C.
a) $\vec{E} \| \vec{C}$ b) $\vec{E}_{\perp} \vec{C}$

Figure 6. SDP at 295°K and $\sim 10^{-3}$ torr 1) before and 2) after heat treatment to 175°C. $\vec{E} \| \vec{C}$.

Figure 7. Effect of 0.85 μm illumination on the SDP at $\sim$ 87°K and $\sim 10^{-3}$ torr. $\vec{E} \| \vec{C}$. Curve 1: without IR; 2) with IR.

Figure 8. Spectral distribution of the quenching of 1) the B-exciton photocurrent and 2) the near band edge photocurrent (4933 Å, $\vec{E} \perp \vec{C}$) at ~ 87°K and 10^{-3} torr. Dashed lines represent the respective bias photocurrent levels.

Figure 9. Kinetic behavior of the excitation of the near band edge peak (4933 Å, $\vec{E} \perp \vec{C}$) at ~ 87°K.

Figure 10. Band model of the active region of a Class I crystal.

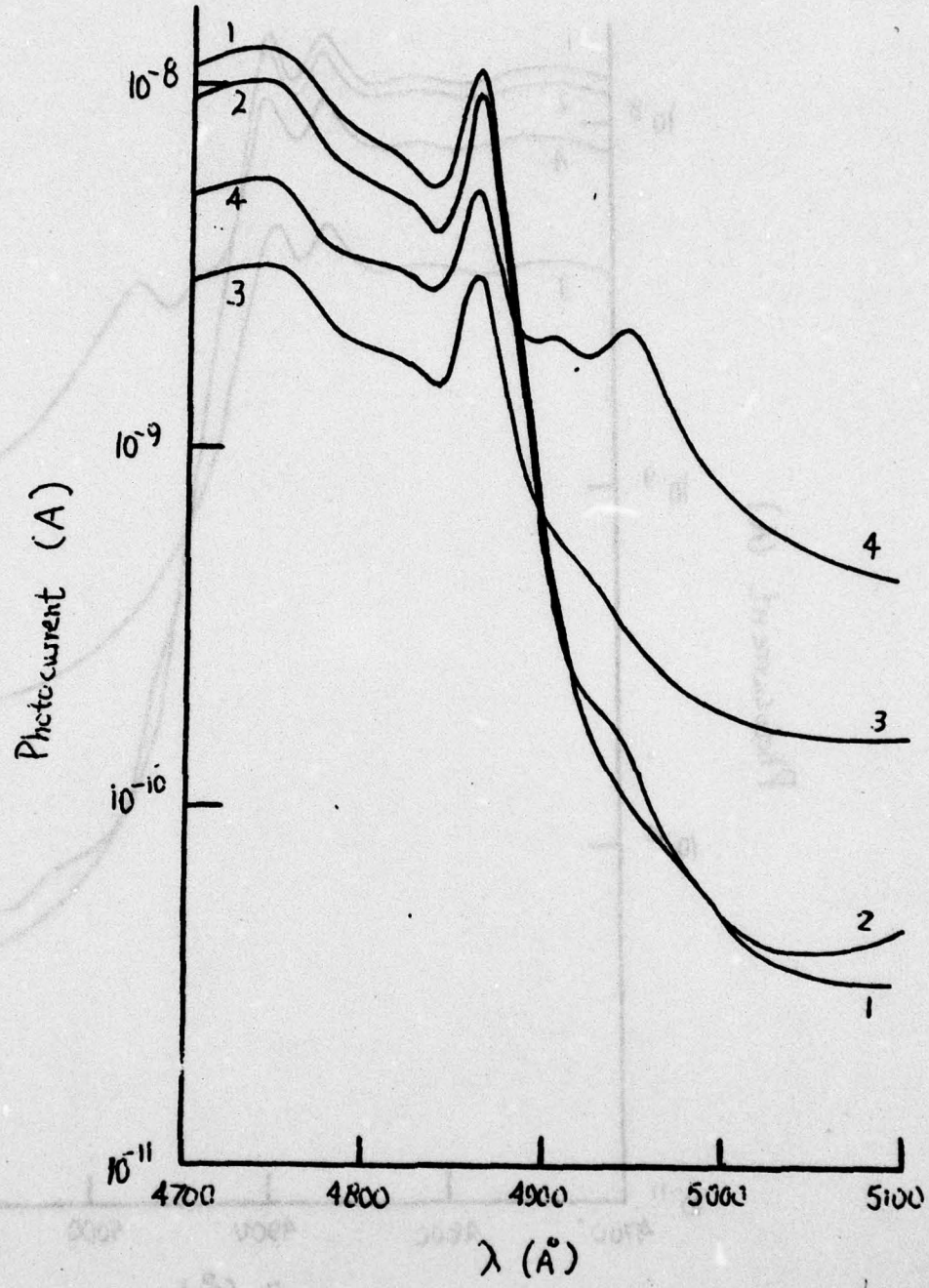
1
2
4
3
10^{-8}
10^{-9}
10^{-10}
10^{-11}
Photocurrent (A)
4700
4800
4900
5000
5100
λ (Å)

Fig. 1a.

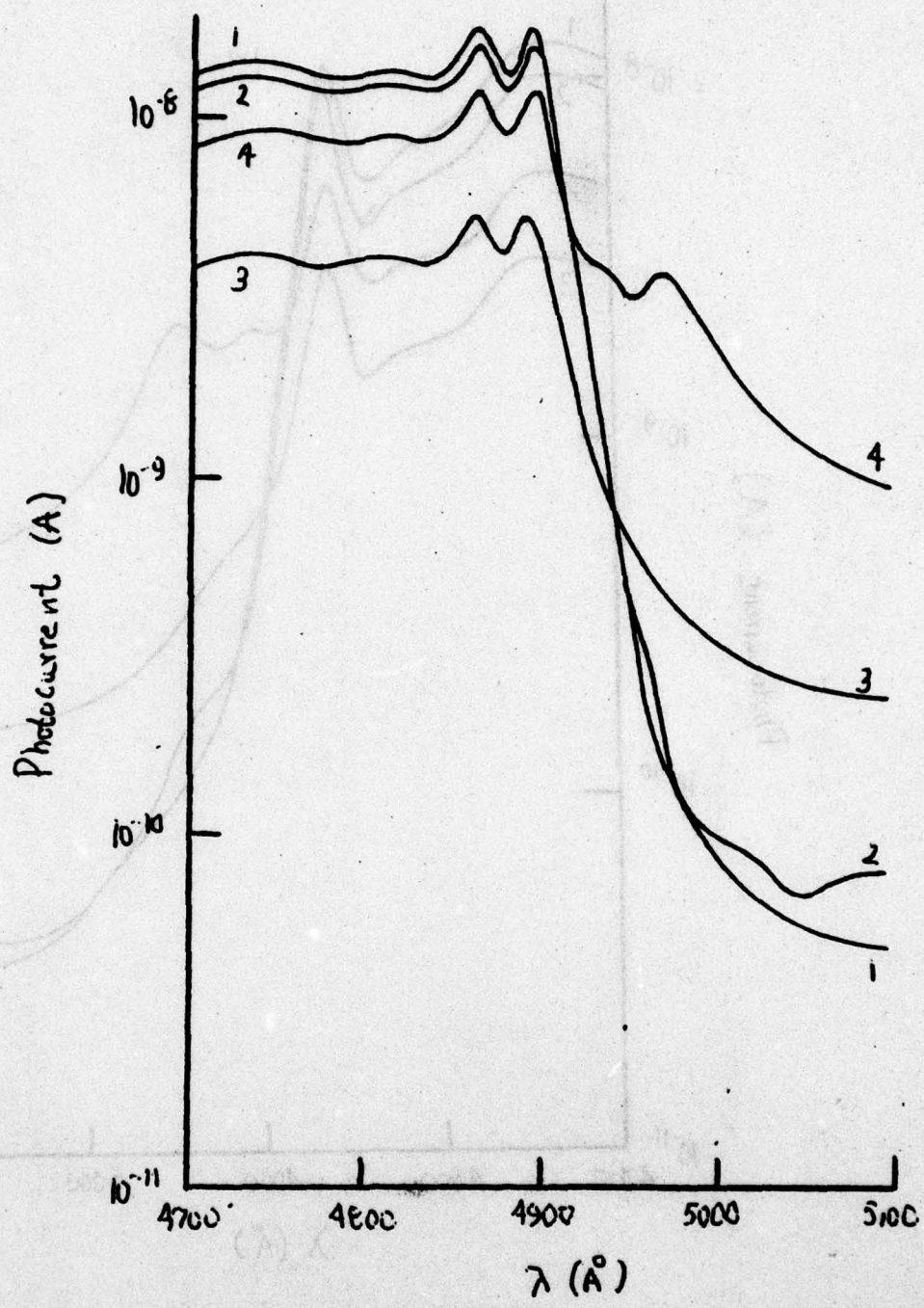
1
2
4
3
10^{-8}
10^{-9}
10^{-10}
10^{-11}
Photocurrent (A)
4700
4800
4900
5000
5100
λ (Å)
4
3
2
1

Figure 1b.

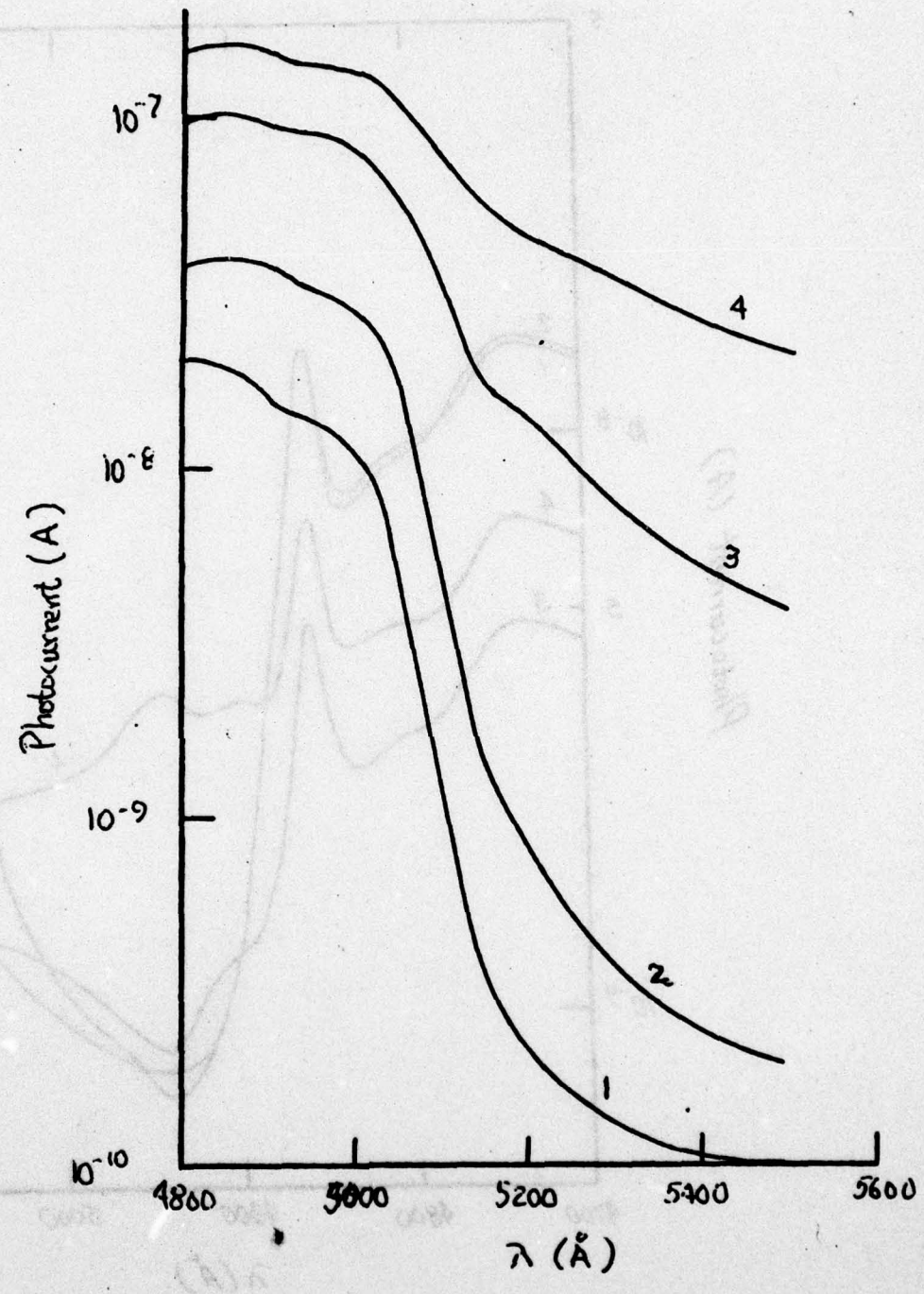
Photocurrent (A)
10⁻⁷
10⁻⁸
10⁻⁹
10⁻¹⁰
4800
5000
5200
5400
5600
λ (Å)
1
2
3
4

Figure 2.

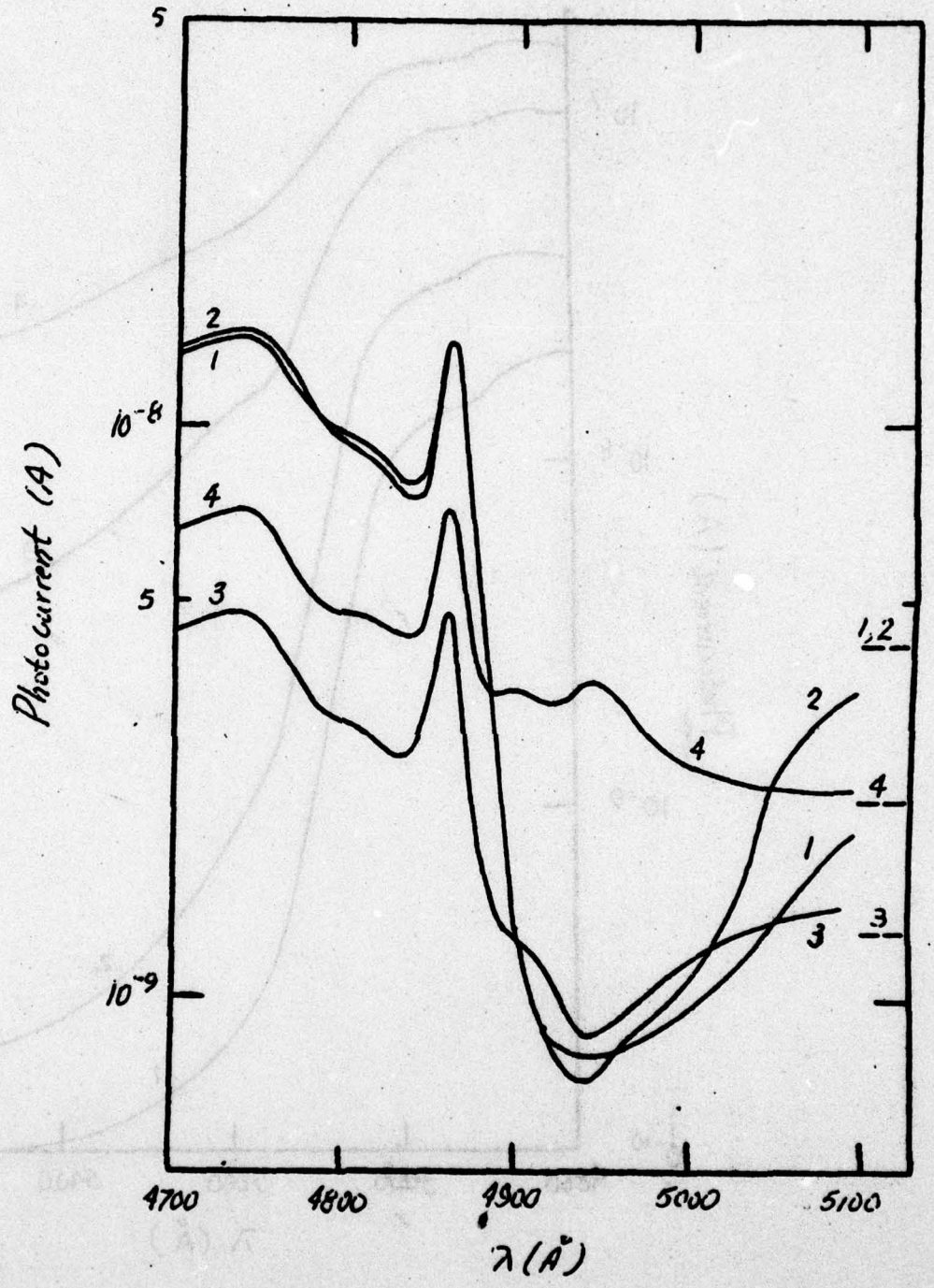
5
2
1
10^{-8}
4
5
3
Photocurrent (A)
1,2
2
4
4
1
3
3
10^{-9}
4700
4800
4900
5000
5100
λ (Å)

Figure 3a

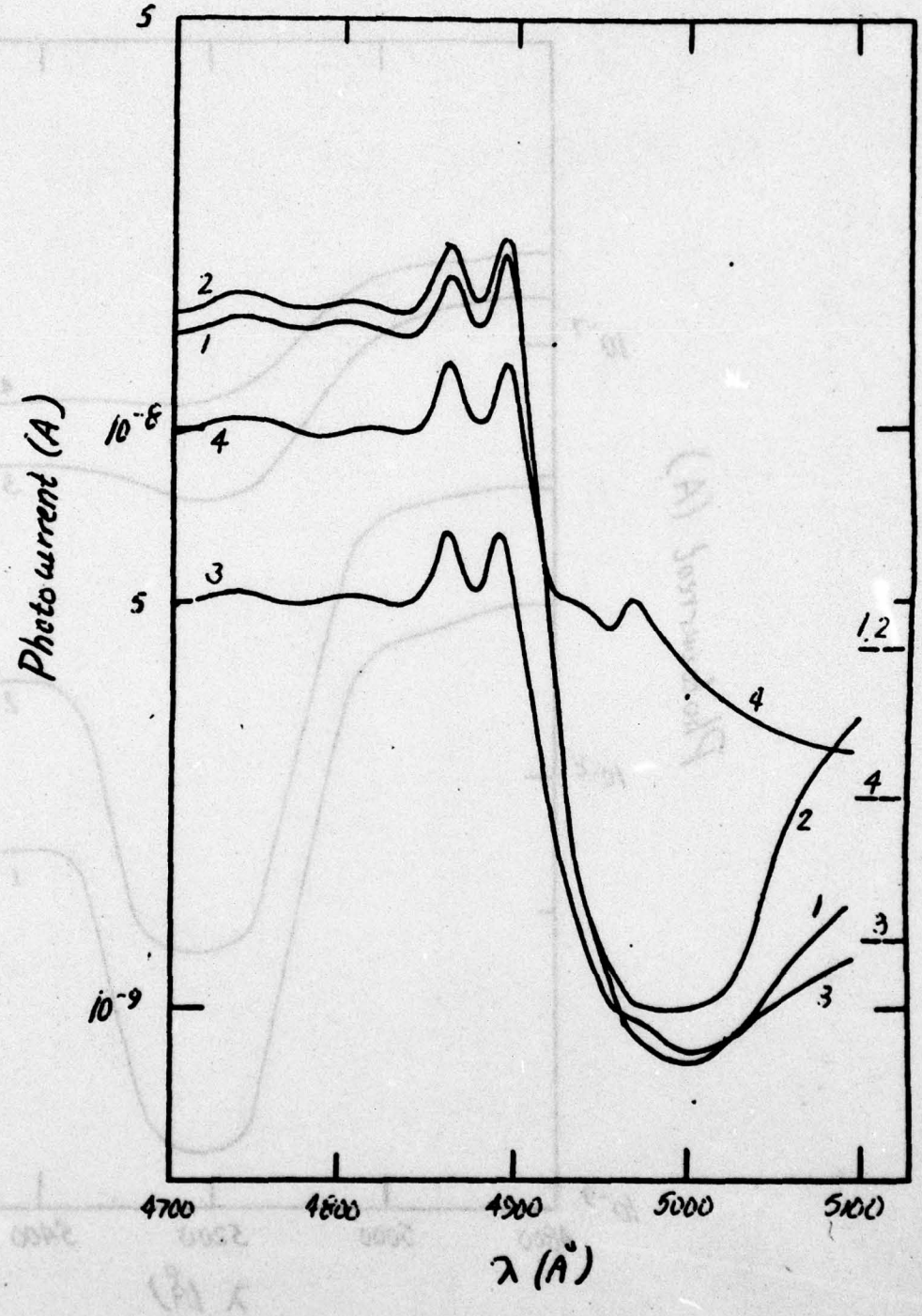
5
10^{-8}
5
10^{-9}
Photocurrent (A)
2
1
4
3
1.2
4
2
1
3
3
4700
4800
4900
5000
5100
λ (Å)

Figure 3b.

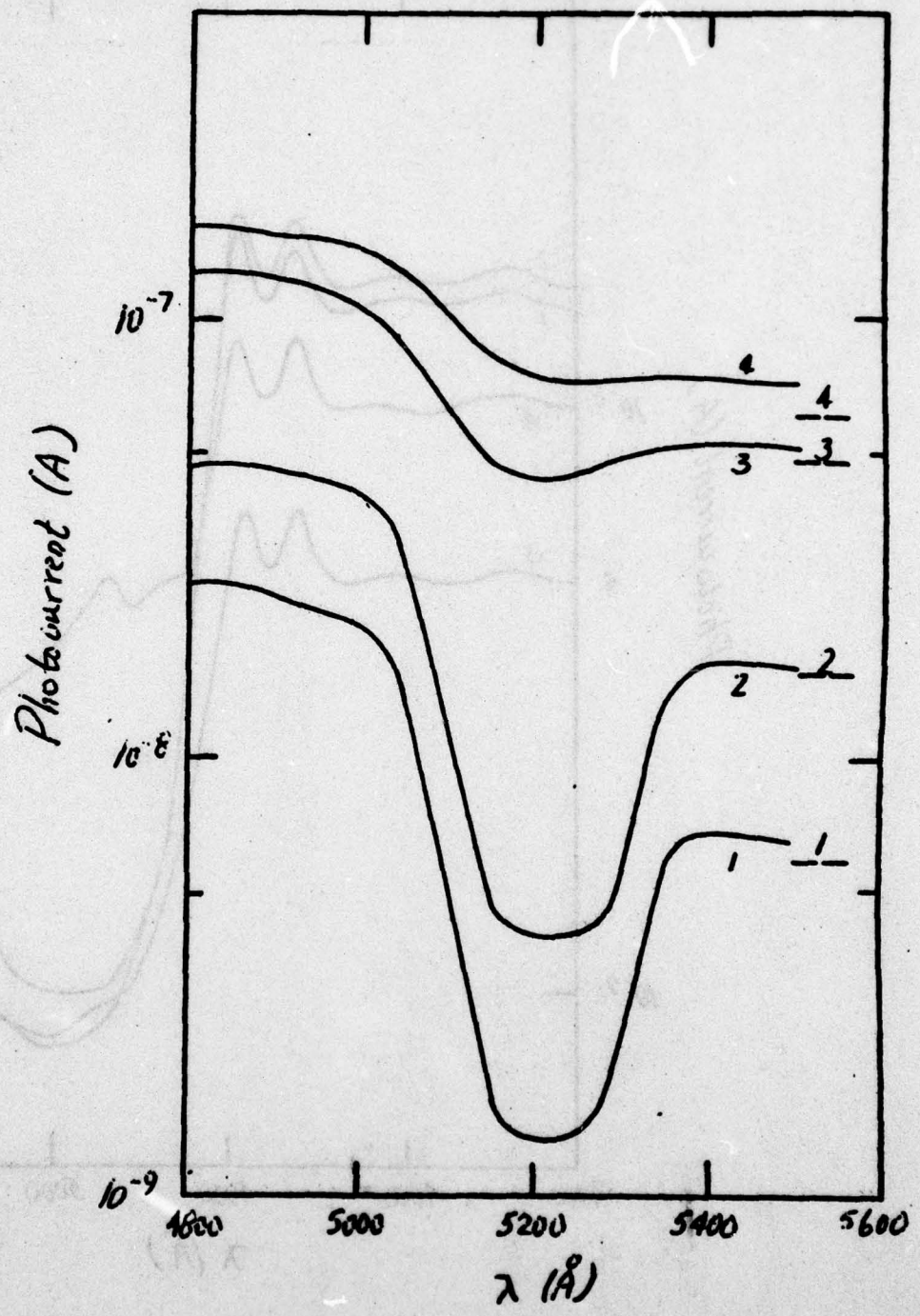
Photocurrent (A)
10^{-7}
10^{-8}
10^{-9}
4
4
3
3
2
2
1
1
4800
5000
5200
5400
5600
λ (Å)

Figure 4.

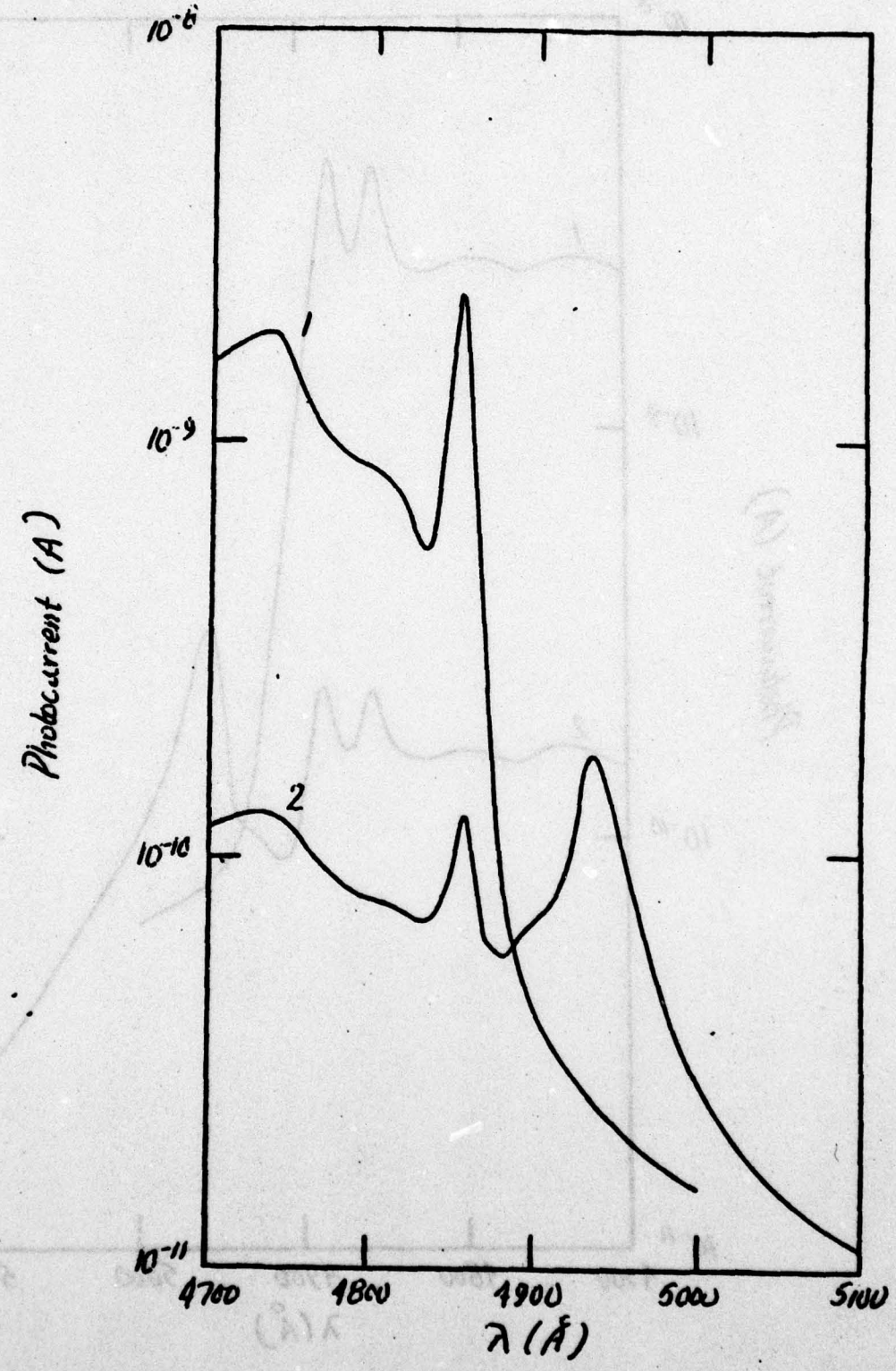
10^{-8}
10^{-9}
10^{-10}
10^{-11}
Photocurrent (A)
1
2
4700
4800
4900
5000
5100
λ (Å)

Figure 5a.

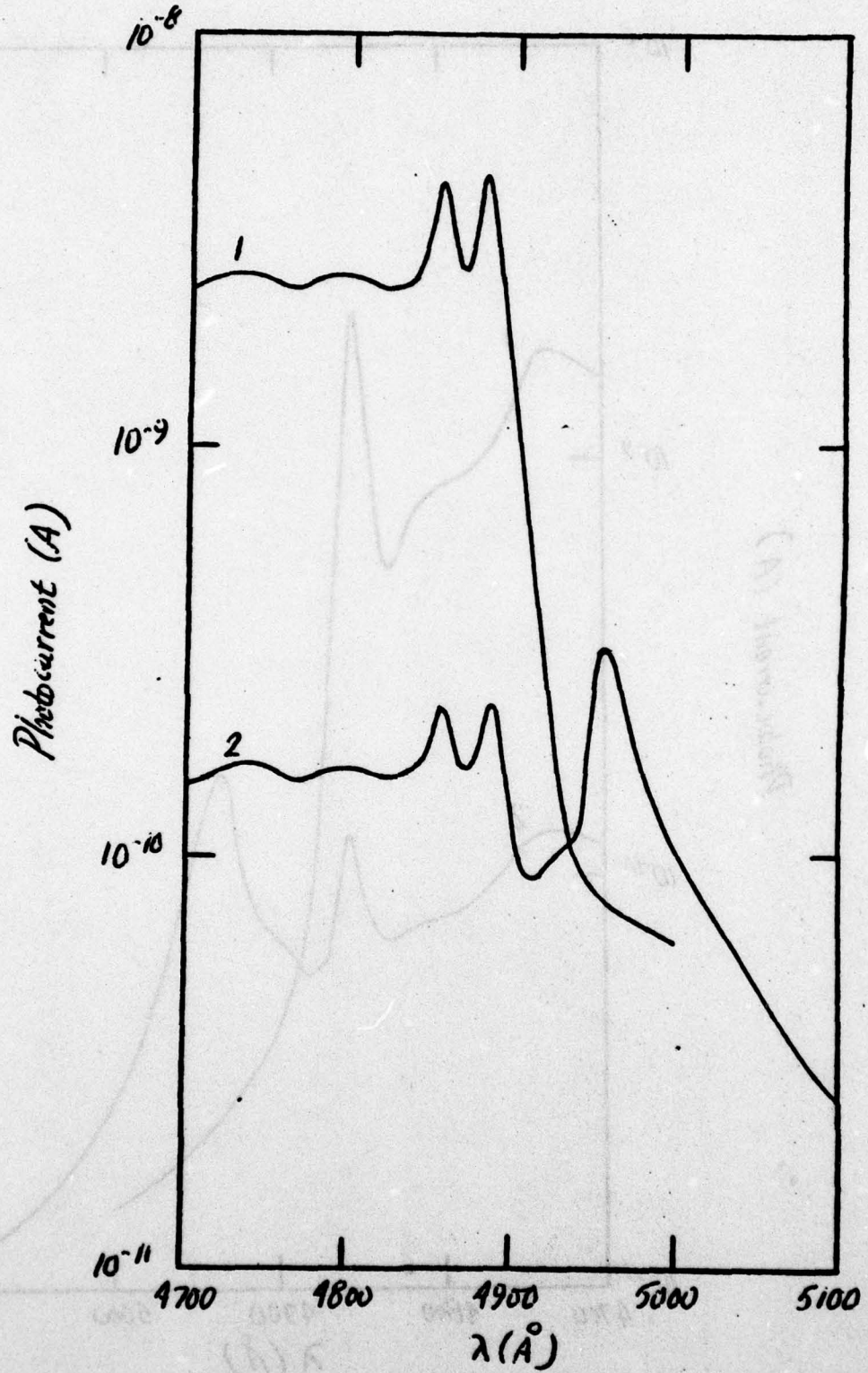
10^{-8}
10^{-9}
10^{-10}
10^{-11}
Photocurrent (A)
1
2
4700
4800
4900
5000
5100
λ(Å)

Figure 5b.

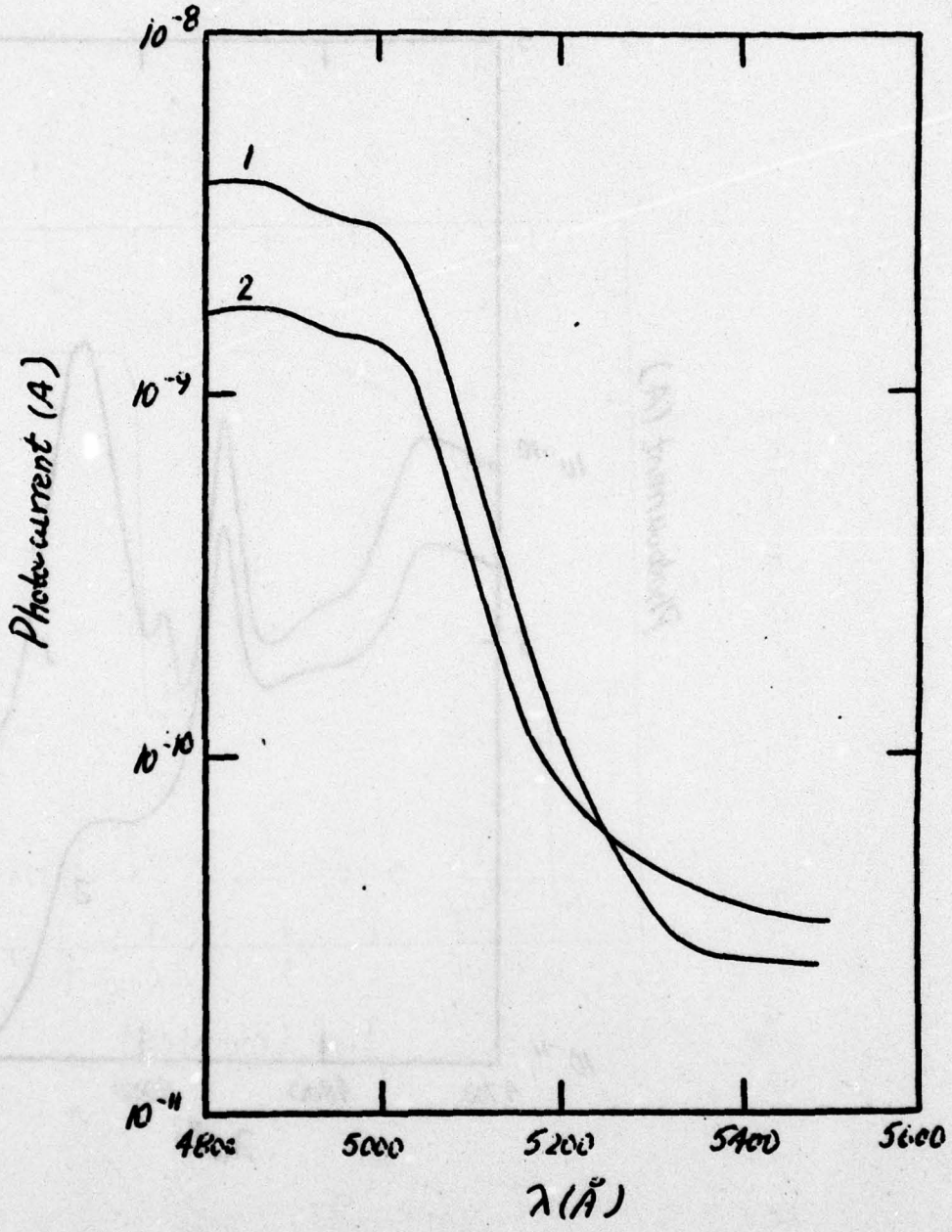
10^{-8}
10^{-9}
10^{-10}
10^{-11}
1
2
Photocurrent (A)
4800
5000
5200
5400
5600
λ(Å)

Figure 6.

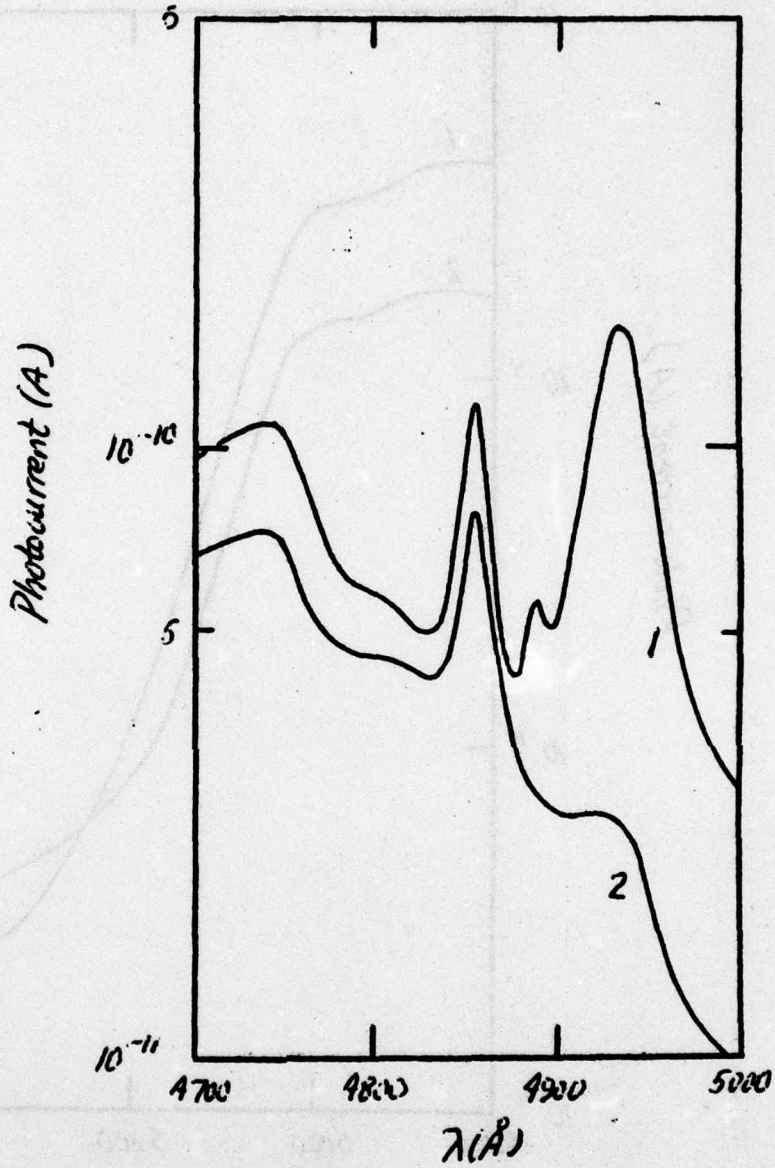

Figure 7

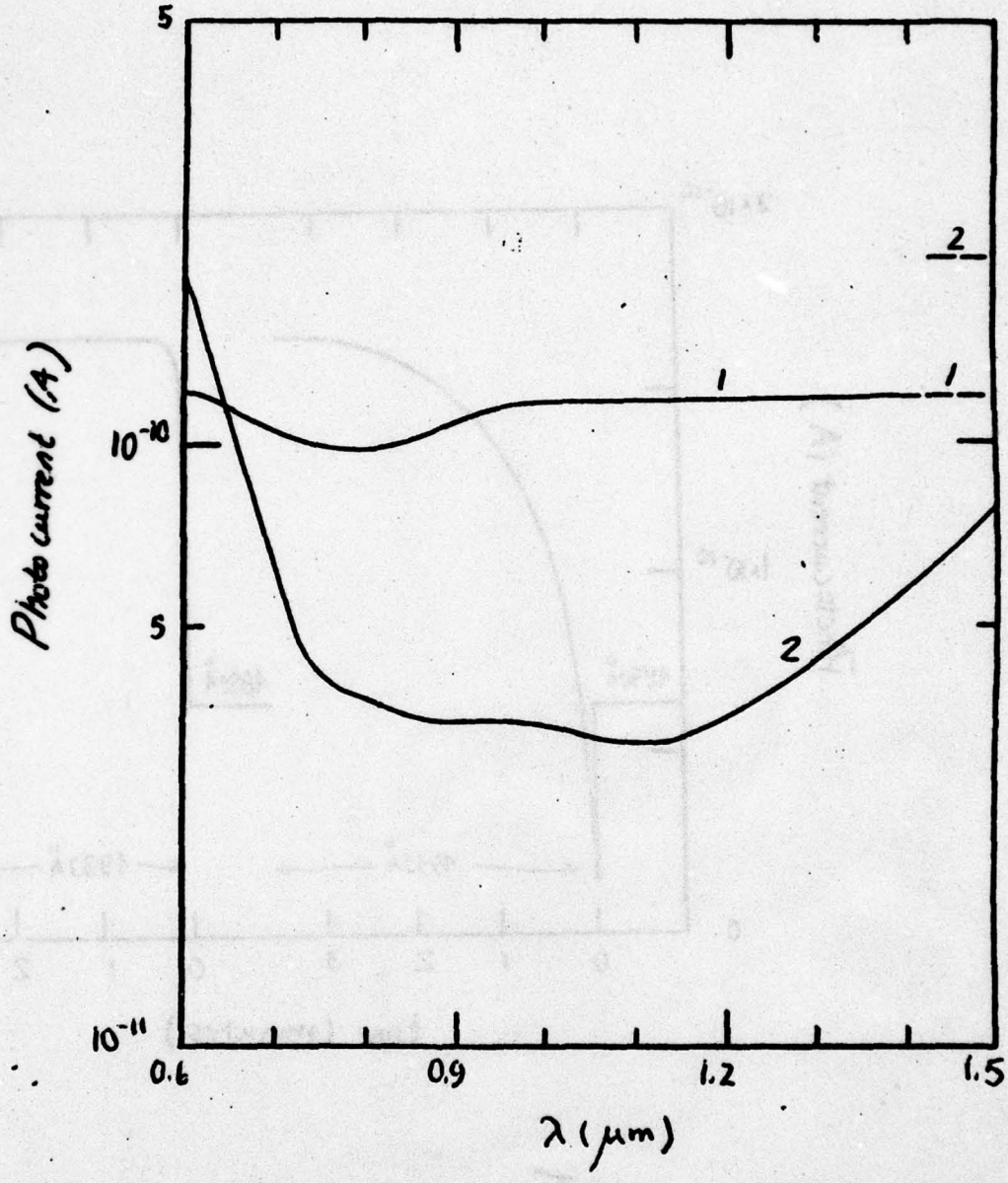

Figure 8.

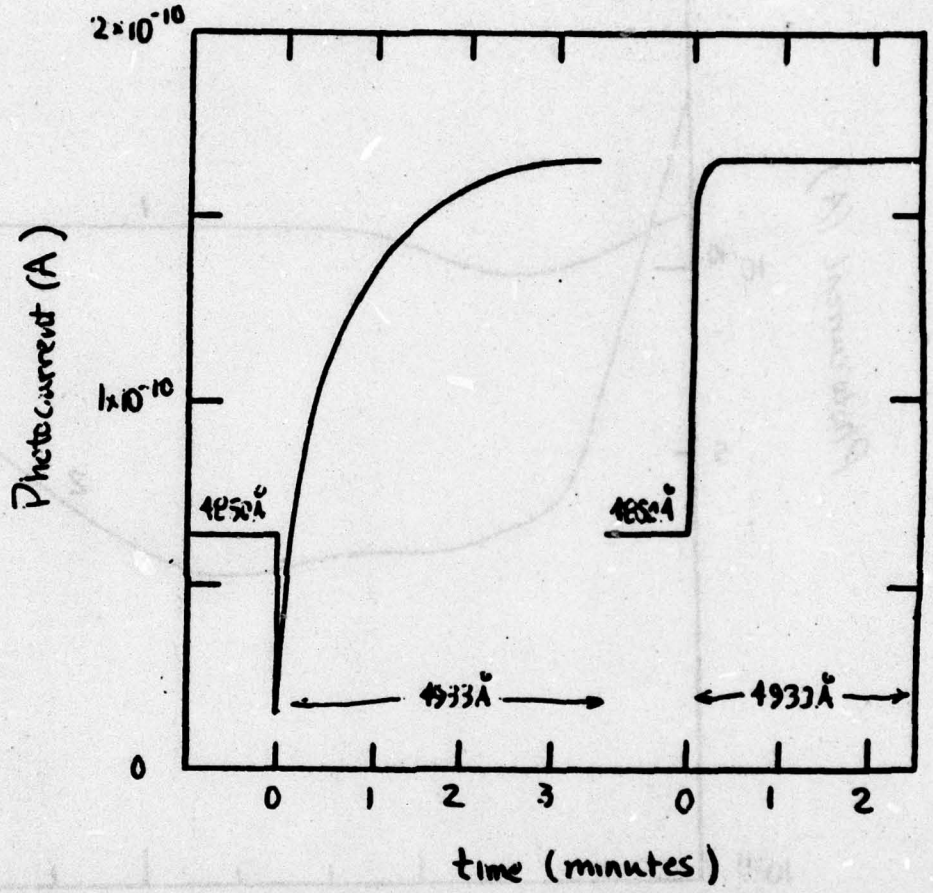
2×10⁻¹⁰
1×10⁻¹⁰
0
Photocurrent (A)
4850Å
4933Å
4933Å
4854Å
0 1 2 3 0 1 2
time (minutes)

Figure 9.

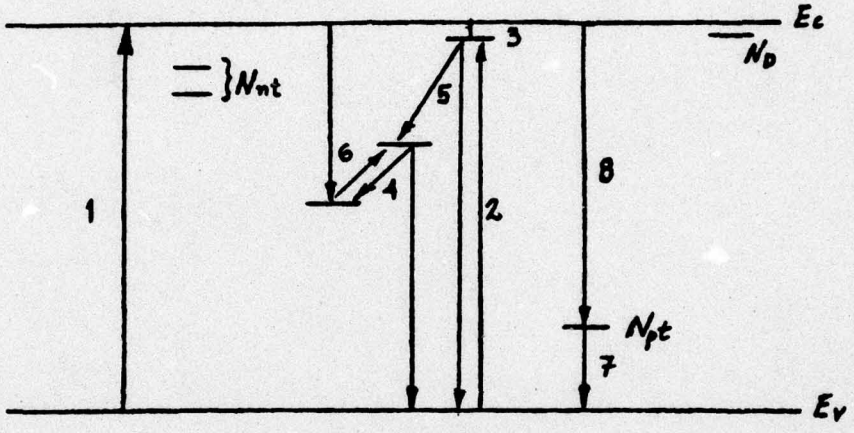
E_c
N_D
N_{nt}
3
5
6
4
1
2
8
N_{pt}
7
E_v
0 -1 -2
CHARGE STATE
OF
MULTI-CHARGED
RECOMBINATION
CENTER